BJ www.biochemj.org

Biochem. J. (2011) **440**, 185–193 (Printed in Great Britain) doi:10.1042/BJ20111243

Intracellular curvature-generating proteins in cell-to-cell fusion

Jean-Philippe RICHARD*[1,2], Evgenia LEIKINA*[1], Ralf LANGEN†, William Mike HENNE‡[3], Margarita POPOVA*, Tamas BALLA§, Harvey T. McMAHON‡, Michael M. KOZLOV‖ and Leonid V. CHERNOMORDIK*[4]

*Section on Membrane Biology, Laboratory of Cellular and Molecular Biophysics, Eunice Kennedy Shriver National Institute of Child Health and Human Development, National Institutes of Health, 10 Center Dr., Bethesda, MD 20892-1855, U.S.A., †Zilkha Neurogenetic Institute and Department of Biochemistry, Keck School of Medicine, University of Southern California, Los Angeles, CA 90033, U.S.A., ‡MRC Laboratory of Molecular Biology, Hills Road, Cambridge CB2 0QH, U.K., §Section on Molecular Signal Transduction, Program for Developmental Neuroscience, National Institute of Child Health and Human Development, National Institutes of Health, Bethesda, MD 20892, U.S.A., and ‖Department of Physiology and Pharmacology, Sackler Faculty of Medicine, Tel Aviv University, 69978 Tel Aviv, Israel

Cell-to-cell fusion plays an important role in normal physiology and in different pathological conditions. Early fusion stages mediated by specialized proteins and yielding fusion pores are followed by a pore expansion stage that is dependent on cell metabolism and yet unidentified machinery. Because of a similarity of membrane bending in the fusion pore rim and in highly curved intracellular membrane compartments, in the present study we explored whether changes in the activity of the proteins that generate these compartments affect cell fusion initiated by protein fusogens of influenza virus and baculovirus. We raised the intracellular concentration of curvature-generating proteins in cells by either expressing or microinjecting the ENTH (epsin N-terminal homology) domain of epsin or by expressing the GRAF1 (GTPase regulator associated with focal adhesion kinase 1) BAR (Bin/amphiphysin/Rvs) domain or the FCHo2 (FCH domain-only protein 2) F-BAR domain. Each of these treatments promoted syncytium formation. Cell fusion extents were also influenced by treatments targeting the function of another curvature-generating protein, dynamin. Cell-membrane-permeant inhibitors of dynamin GTPase blocked expansion of fusion pores and dominant-negative mutants of dynamin influenced the syncytium formation extents. We also report that syncytium formation is inhibited by reagents lowering the content and accessibility of PtdIns(4,5)P_2, an important regulator of intracellular membrane remodelling. Our findings indicate that fusion pore expansion at late stages of cell-to-cell fusion is mediated, directly or indirectly, by intracellular membrane-shaping proteins.

INTRODUCTION

Cells fuse in developmental processes, such as fertilization, muscle and bone formation, and in pathological processes, including viral infections and carcinogenesis [1–5]. Early stages of membrane fusion driven by specialized protein fusogens [2,6–8] culminate in the opening of nanometre-sized fusion pores that connect the volumes of the two cells [9–11]. The mechanisms that drive subsequent expansion of the fusion pore(s) to a micrometre-sized lumen that allows complete coalescence of cytoplasms are poorly understood. In our recent studies, to uncouple later fusion stages from earlier ones, we explored syncytium formation initiated by well-characterized viral envelope proteins: influenza virus HA (haemagglutinin) [12] and baculovirus gp64 [13]. Both HA- and gp64-mediated fusion processes are triggered by treating HA- or gp64-expressing cells with a low pH medium that mimics conditions in acidified endosomes during viral entry. In these fusion processes, the opening of nascent fusion pores develop much faster than their expansion to sizes detectable by light microscopy (0.1–1 s compared with tens of min for gp64 [14]; 1 min compared with 1–2 h for HA [12,15]). Relatively fast and thus almost synchronous opening of fusion pores after low pH application facilitates analysis of the slower process of fusion pore expansion. Using these experimental systems we have established that, in contrast with fusion pore opening, pore expansion and thus syncytium formation are blocked by ATP depletion, indicating that pore growth is not spontaneous, but is rather driven by cell machinery [12,13]. Several studies have proposed that the expansion of fusion pores in cell fusion is driven by the cytoskeleton [16–18]. However, modifications of the microtubule cytoskeleton have no effect on syncytium formation initiated by viral fusogens [12], and depolymerization of actin cytoskeleton promotes rather than inhibits syncytium formation, suggesting that actin structures restrict rather than drive fusion pore expansion [12,13,19].

As long as the fusion pore grows within the tight contact zone, the membrane bilayer at the edge of the pore remains strongly curved and, hence, accumulates the elastic energy of bending (Figure 1, inset). In the course of fusion pore expansion, the length of the pore edge grows and thus the elastic energy increases. The degree of membrane bending at the pore rim is similar to that of intracellular membrane structures such as membrane tubules and endocytic vesicles [20,21], all characterized by the curvature radii of a few tens of nanometres. Therefore our search for protein machinery that can power syncytium formation has focused on the cytosolic proteins involved in the cell-controlled bending of intracellular membranes. CGPs (curvature-generating proteins), such as dynamin [22–24], ENTH (epsin N-terminal

Abbreviations used: BAR, Bin/amphiphysin/Rvs; cELISA, cell surface ELISA; CGP, curvature-generating protein; DMEM, Dulbecco's modified Eagle's medium; EGFP, enhanced green fluorescent protein; ENTH, epsin N-terminal homology; FCHo2, FCH domain-only protein 2; GFP, green fluorescent protein; GRAF1, GTPase regulator associated with focal adhesion kinase 1; HA, haemagglutinin; MiTMAB, tetradecyl trimethylammonium bromide; MOI, multiplicity of infection; PH, pleckstrin homology; PLCδ1PH, PH domain of phospholipase Cδ1.

[1] These authors contributed equally to this work

[2] Present address: Hugo W. Moser Research Institute at Kennedy Krieger, Department of Neurology, Johns Hopkins School of Medicine, Baltimore, MD 21205, U.S.A.

[3] Present address: Weill Institute for Cell and Molecular Biology, Cornell University, Ithaca, NY 14853, U.S.A.

[4] To whom correspondence should be addressed (email chernoml@mail.nih.gov).

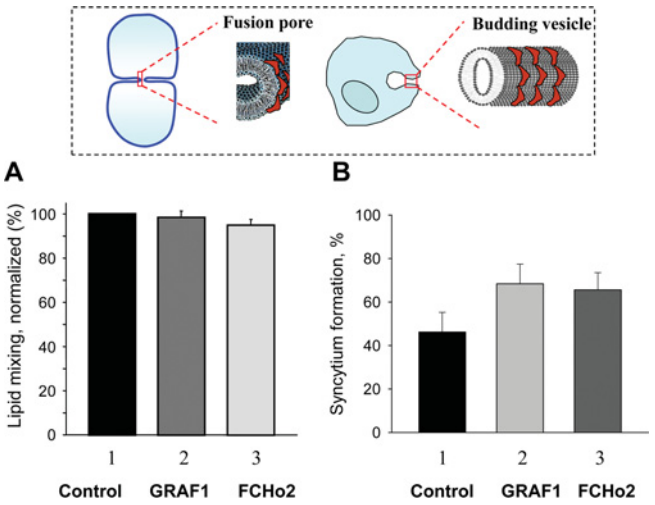

Figure 1 Overexpression of the F-BAR domain of FCHo2 and the N-BAR domain of GRAF1 in HAb2 cells does not affect HA-mediated early fusion stages (lipid mixing, A), but promotes syncytium formation (B)

The inset shows a similarity between membrane curvatures in the semi-cylindrical rim of the fusion pore connecting two cells and in membrane tubules and endocytic vesicles formed by intracellular curvature-generating proteins (red shapes). (**A** and **B**) Cells were transfected with an EGFP plasmid containing the BAR and PH domains of GRAF1 (2) or the F-BAR domain (amino acids 1–272) domain of FCHo2 (3). (1) Control with mock-transfected cells. (**A**) Local fusion was monitored by following the rate of mixing of membrane dye PKH26 from a labelled ghost erythrocyte to an unlabelled HAb2 cell. Lipid-mixing extents were normalized to those in the control experiments. Results are means + S.E.M. ($n \geqslant 3$). (**B**) The final extents of syncytium formation were recorded 2 h after initiation of fusion. Results are means + S.E.M. This graph represents five out of six experiments. One experiment failed to give us appropriate control data and was withdrawn from the data collection. The differences between syncytium formation extents for the cells transfected with either the GRAF1 or FCHo2 constructs and mock-transfected cells were statistically significant ($P = 0.019$ and $P = 0.007$ respectively, paired Student's t test).

homology) domain proteins (e.g. epsin 1 [25,26]) and BAR (Bin/amphiphysin/Rvs) domain proteins such as GRAF1 (GTPase regulator associated with focal adhesion kinase 1) [27–29] and F-BAR proteins including FCHo2 (FCH domain-only protein 2) [25,30] are recruited to membranes, often by protein interaction with PtdIns(4,5)P_2, play an essential role in intracellular processes involving membrane remodelling [31]. We have previously hypothesized that these proteins may accumulate at the fusion pore rim, lower its energy and thus promote pore expansion and syncytium formation [13]. In principle, CGPs can also promote late stages of syncytium formation by driving vesiculation of membrane material in the vicinity of fusion pore(s) suggested as a possible mechanism of pore growth [32,33]. However, other studies suggest that fusion pore expansion does not involve vesiculation [13,34].

In the present study we explored whether the efficiency of the late stages of cell–cell fusion initiated by influenza HA and baculovirus gp64 depends on the activity of intracellular CGPs. Analysis of possible mechanisms of such dependence and identification of specific CGPs involved in biologically relevant cell fusion processes will be examined in future work. We modified the activity of the BAR, F-BAR and ENTH domains of several proteins by either transfecting the cells to express these protein active domains or by microinjecting the domains into cells. To minimize indirect effects, we used constructs lacking protein domains which are responsible for interactions with other proteins but not required for membrane shaping. We found that the GRAF1 BAR domain, the FCHo2 F-BAR domain and the epsin ENTH domain promote cell fusion. Late stages of fusion were affected by PtdIns(4,5)P_2-targeting reagents and by modifying the functional activity of dynamin either by expressing different dynamin mutants or by blocking dynamin GTPase activity with cell-membrane-permeant inhibitors. The finding that changes in the concentration and/or activity of diverse proteins involved in shaping intracellular membranes and in the membrane concentration of accessible PtdIns(4,5)P_2, an important regulator of membrane shaping, affect late fusion stages substantiates the hypothesis that CGPs drive fusion pore expansion in cell-to-cell fusion.

EXPERIMENTAL

Reagents and plasmids

Dynasore [35] was first supplied by Dr T. Kirchhausen (Harvard University, Boston, MA, U.S.A.) and then purchased from Sigma. Another dynamin inhibitor, MiTMAB (tetradecyl trimethylammonium bromide) [36], was also purchased from Sigma. Dynole-34-2 and its inactive derivative Dynole-31-2, used as a negative control [37], were purchased from Ascent Scientific. Dynasore [35], MiTMAB [36] and Dynoles [37] were applied as described previously. Polyphosphoinositide-binding peptide PBP10, a rhodamine B-tagged ten-residue peptide derived from the PtdIns(4,5)P_2-binding region in segment 2 of gelsolin [38] was purchased from EMD Millipore and was used as suggested by the manufacturer. Alexa Fluor® 594-conjugated 10000 Da dextran was purchased from Invitrogen.

We also used pEGFP [enhanced GFP (green fluorescent protein)] plasmids containing either the rat ENTH domain of epsin (amino acids 1–164) or its mutant L6E, the F-BAR domain of mouse FCHo2 (amino acids 1–272) or the BAR and PH (pleckstrin homology) domains of GRAF1 (amino acids 1–382). To evaluate PtdIns(4,5)P_2 content in the plasma membrane and to compete for PtdIns(4,5)P_2 binding with endogenous PtdIns(4,5)P_2-binding proteins, we expressed PLCδ1PH (PH domain of phospholipase Cδ1)–GFP construct or, in control experiments, its inactive mutant (R40L) construct, which does not bind to the plasma membrane [39]. The recombinant ENTH domain of epsin1 was expressed and purified as described previously [25]. Wild-type baculovirus AcNPV was purchased from Invitrogen. Baculoviruses encoding several dominant-negative dynamin mutants of human neuronal dynamin-1 (S61D [40], I690K [41], K44A [42] and S45N [43,44]) were provided by Dr S. Schmid (Department of Cell Biology, The Scripps Research Institute, La Jolla, CA, U.S.A.). PKH26 was purchased from Sigma.

Cell culture and preparation

HAb2 cells (NIH 3T3 cells stably expressing HA) were cultured as exponentially growing subconfluent monolayers on 90 mm plates in DMEM (Dulbecco's modified Eagle's medium) supplemented with Glutamax (Invitrogen) and 10 % (v/v) fetal bovine serum. Exponentially growing cells were dissociated with trypsin (Invitrogen). The cells (2.5×10^5) were plated and cultured overnight on 30 mm plates. In some experiments, human erythrocyte ghosts were labelled with fluorescent lipid PKH26 (Sigma) as described previously [45].

Spodoptera frugiperda (Sf9) cells and Sf9^{Op1D} cells, i.e. stably transfected Sf9 cells expressing a protein fusogen of baculovirus OpMNPV gp64 [14,46], provided by Dr Gary Blissard (Cornell University, Ithaca, NY, U.S.A.), were grown and, in some experiments, labelled with L-α-phosphatidylethanolamine-*N*-(lissamine rhodamine B sulfonyl) (egg) (Rho-PE, Avanti Polar Lipids) as described previously [13,47].

Transfection

Transfections were performed using Lipofectamine™ 2000 (Invitrogen) using the protocol suggested by the manufacturer. Fusion was triggered 24 h after transfection.

Infection with baculovirus constructs

To drive high levels of mutant dynamin expression in Sf9 cells, we infected the cells with different recombinant baculoviruses or with wild-type baculovirus at an MOI (multiplicity of infection) of 1–10 plaque-forming units per cell. We have adjusted the MOI used for each recombinant baculovirus and for wild-type baculovirus to achieve the same level of expression of baculovirus gp64 at the cell surface, as verified 2 days post-infection by Western blotting of cell-surface gp64 isolated using surface biotinylation and streptavidin beads [48] and by a cELISA (cell surface ELISA) using antibody AcV1 (Santa Cruz Biotechnology) [48]. The levels of expression of exogenous dynamin were similar between different constructs and much higher than the level of endogenous expression of dynamin in Sf9 cells, as verified using Western blotting with the anti-dynamin antibody Hudy 1 (Upstate Biotechnology). We have also confirmed that the cells infected with all of the recombinant baculoviruses used were expressing similar amounts of different dynamin mutants, which were much higher than the amounts of endogenous dynamin observed for non-infected cells.

Microinjection

The microinjection experiments were performed on a Zeiss Axiovert135 with a FemtoJet and InjectMan NI2 (Eppendorf). The microinjected solution was composed of 1 vol. of Alexa Fluor® 594-tagged 10000 Da dextran (5 mg/ml in double-distilled water] (Invitrogen), 1 vol. of the protein of interest, 2 vol. of double-distilled water and 1 vol. of microinjection buffer (250 mM Hepes, pH 7.2, 500 mM KCl and 25mM Na_2HPO_4). In each microinjection experiment, we injected 20 out of 30–40 cells per field of view with either fluorescent dextran alone or fluorescent dextran mixed with the protein of interest (the average fraction of injected cells per field was 50–70 %) and five fields per condition (total of 100 injected cells).

Application of dynamin inhibitors and PtdIns(4,5)P_2-targeting reagent

The GTPase activity of dynamin in HAb2 and $Sf9^{Op1D}$ cells was inhibited by treating the cells with dynasore, Dynole-34-2 and MiTMAB. The reagents were applied either before (for 30 min) or immediately after low pH application (for 20 min). Dynole-34-2 and its inactive analogue Dynole-31-2 were both applied to $Sf9^{Op1D}$ cells for 20 min immediately after a 1 min application of pH 4.9 medium. PBP10, butan-1-ol and *t*-butanol were both applied to $Sf9^{Op1D}$ cells for 15 min immediately after a 1 min application of pH 4.9 medium.

Fusion assays

In all of the results presented, the syncytium index for each condition was determined as the number of nuclei in a multinucleated cell divided by the total number of nuclei in the field [12]. As verified in Supplementary Figure S1 at (http://www.BiochemJ.org/bj/440/bj4400185add.htm), an inhibitor (Dynole 34-2) that lowered the percentage of nuclei in multinucleated $Sf9^{Op1D}$ cells also shifted the distribution of the number of nuclei per cell towards cells with lower number of nuclei.

Fusion between HAb2 cells was assayed as described previously [12]. In brief, HAb2 cells were pre-treated with trypsin (5 μg/ml, 5 min and 37 °C) to cleave HA into the fusion-competent conformation. Then the cells were washed once with PBS with Ca^{2+}/Mg^{2+} and once with pH 4.9 medium, and then exposed for 5 min to pH 4.9 medium at 37 °C, in order to trigger the fusogenic conformational change in HA. Cells were washed two more times with PBS and incubated at 37 °C for 2 h in DMEM supplemented with serum. Cells were scored as syncytia if they had multiple nuclei in a single cell volume or if the connections between fusing cells appeared to be large enough to allow the nucleus passage. In some experiments, in order to evaluate the efficiency of early fusion stages, the extents of lipid mixing between HAb2 cells and PKH26-labelled erythrocytes were measured as the ratio of dye redistributed from bound erythrocytes to the total number of bound erythrocytes [45].

Fusion between $Sf9^{Op1D}$ cells and between baculovirus-infected Sf9 cells was assayed as described previously [13]. In brief, fusogenic activity of gp64 was triggered at 22 °C by a 5 min application of Grace medium with pH adjusted to 4.9. At 30 min after re-neutralization, the percentage of Sf9 cells or $Sf9^{Op1D}$ cells in syncytia (the ratio of nuclei within syncytia to the total number of cell nuclei in the same field) was scored using light microscopy [47]. Lipid mixing between either Sf9 cells or $Sf9^{Op1D}$ cells was quantified as Rho-PE transfer from labelled to unlabelled cells [13].

In the microinjection experiments, 15–30 min after the microinjection we determined the number of surviving Alexa Fluor® 594-labelled mononucleated cells with nuclei labelled with Hoechst. The fusion was then induced by a 5 min application of pH 4.9 medium at 37 °C. At 2 h after inducing fusion, we scored the efficiency of syncytium formation (P_{fc}, percentage of fused injected cells) by determining the percentage of Alexa Fluor® 594-labelled mononucleated cells that remained mononucleated (and thus unfused cells, P_{ufc}). Since the trauma of injection may influence the fusion rate of injected cells compared with non-injected cells, cell fusion efficiency for the cells injected with protein of interest, which was determined using the expression $P_{fc} = 100 - P_{ufc}$, was compared with that for the cells injected with dextran only.

In the experiments aimed at exploring the effects of the expression of the PLCδ1PH–GFP construct, we focused on transfected $Sf9^{Op1D}$ cells. We quantified the efficiency of syncytium formation by dividing the number of nuclei in GFP-labelled (green) multinucleated cells in the field of view by the total number of nuclei in GFP-labelled cells (both mono- and multi-nucleated cells). The efficiency was then normalized to that observed in a parallel experiment on the cells transfected with the inactive mutant R40L that does not bind PtdIns(4,5)P_2 in the plasma membrane [39].

Each experiment of the present study was repeated at least three times and all functional dependencies reported were observed in each independent experiment. Statistical analysis was carried out using SigmaPlot for Windows, version 11.0.

RESULTS

The F-BAR domain of FCHo2 and the BAR domain of GRAF1 promote syncytium formation

To explore whether CGP domains of FCHo2 and GRAF1 affect HA-initiated syncytium formation, we transfected HAb2 cells with constructs containing either the F-BAR domain of FCHo2 [30,49] or the BAR domain and PH domain of GRAF1 [27,28]. Early stages of HA-mediated fusion were unaffected by the

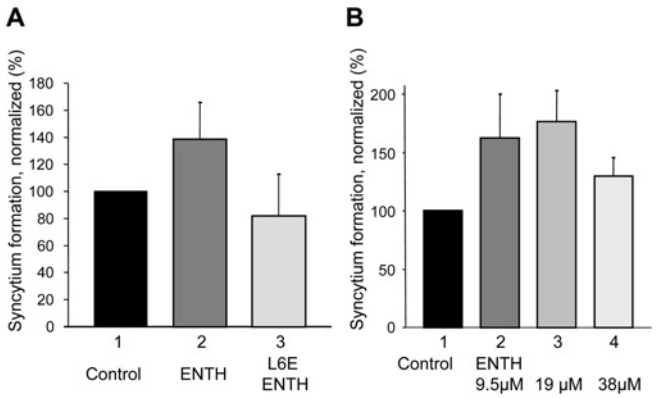

Figure 2 Effects of the ENTH domain of epsin on HA-initiated syncytium formation

(**A**) Cells were transfected with an EGFP plasmid containing the wild-type ENTH domain of epsin (2) or the mutant L6E (3). (1) Control with mock-transfected cells. (**B**) Cells were microinjected with Alexa Fluor® 594-conjugated dextran and microinjection buffer without (1) or with (2, 3 and 4) the ENTH domain of epsin at different concentrations (9.5 μM, 19 μM and 38 μM respectively). Low pH medium inducing fusion was applied 15–30 min after microinjection. Not-normalized fusion extents for the cells injected with 19 μM ENTH domain and the cells injected with only 10 kDa dextran were significantly different (paired Student's t test, $P < 0.001$, $n = 6$). For (**A**) and (**B**), the final extents of fusion were measured 2 h after the end of low pH application and normalized to those in the control experiments. Results are means + S.E.M. ($n \geqslant 3$).

transfection, as shown by the same efficiency of lipid mixing between PKH26-labelled RBCs and either control or transfected HAb2 cells (Figure 1A). However, expression of these CGP domains increased the efficiency of HA-initiated syncytium formation (Figure 1B), indicating that CGPs promote the late stages of cell-to-cell fusion.

The ENTH domain of epsin promotes syncytium formation

The ENTH domain of epsin is also known to induce membrane curvature. We used two experimental approaches, transfection and microinjection, to test the effects of this domain on HA-initiated syncytium formation. In two out of three experiments, we found the extent of HA-mediated syncytium formation to be somewhat higher for HAb2 cells transfected to express the ENTH domain of epsin1 linked to EGFP than for the mock-transfected cells (Figure 2A). However, in one of the experiments we observed no difference in the syncytium formation for transfected and mock-transfected cells. Expression of an ENTH domain of the epsin1 mutant L6E, which is still able to bind to membranes but is defective in membrane bending [25], did not affect syncytium formation.

In another approach, we microinjected 19 μM of the recombinant ENTH domain of epsin1 and observed a statistically significant promotion of syncytium formation compared with mock-injected cells (46 ± 7.8 % compared with 30.3 ± 7.5 %, values are means $\pm$ S.E.M., $n = 6$, $P < 0.001$ in a paired Student's t test). Although some promotion of cell fusion was also observed in the three experiments where we injected 9.5 or 38 μM ENTH domain, the differences between normalized extents of syncytium formation were not statistically significant (Figure 2B). A somewhat weaker promotion of cell fusion at 38 compared with 19 μM of the ENTH domain may reflect the toxicity of the injected protein. Note that, in contrast with early fusion stages, syncytium formation strongly depends on metabolic activity of the fusing cells [12,13].

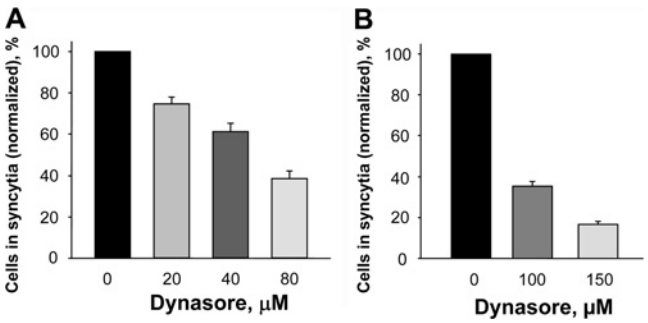

Figure 3 Blocking dynamin GTPase activity with dynasore inhibits syncytium formation initiated by either gp64 (A) or HA (B)

(**A**) Sf9^{Op1D} cells were treated with dynasore at a final concentration of 20 μM, 40 μM or 80 μM before low pH application. (**B**) HAb2 cells were treated with dynasore at a final concentration of 100 μM or 150 μM before low pH application. For (**A**) and (**B**), the final extents of fusion were measured 2 h after the end of low pH application and normalized with those in the control experiments. Results are means + S.E.M. ($n \geqslant 3$).

Dynamin and the late stages of fusion events

The GTPase dynamin, a key player in budding and scission of intracellular vesicles, is one of the most abundant cytosolic CGPs [22,50]. We explored a possible involvement of this protein in the syncytium formation mechanism using three inhibitors of dynamin GTPase activity and by expression of dynamin mutants. Dynasore, a cell-membrane-permeant inhibitor of dynamin GTPase activity [35], inhibited both gp64-initiated syncytium formation by Sf9^{Op1D} cells and HA-initiated syncytium formation by HAb2 cells (Figure 3). Figure 4 shows the inhibition of syncytium formation by Sf9^{Op1D} cells when the low pH application was followed by the application of another cell-permeant dynamin inhibitor Dynole-34-2 that targets an allosteric site at the GTPase domain. Dynole-34-2 lowered both the percentage of nuclei in multinucleate cells (Figure 4) and the sizes of the syncytia (assayed as the distribution of the numbers of nuclei per cell; Supplementary Figure S2 at http://www.BiochemJ.org/bj/440/bj4400185add.htm). No inhibition was observed in the presence of Dynole-31-2, an inactive analogue of Dynole-34-2 [37].

Another cell-membrane-permeant inhibitor of dynamin GTPase, MitMAB, that acts by targeting dynamin interactions with anionic phospholipids [36], also significantly inhibited gp64- or HA-initiated syncytium formation (Figure 5). MiTMAB is a reversible dynamin inhibitor [36], and washing Sf9^{Op1D} cells to remove MiTMAB restored the ability of cells to form syncytia (Figure 5A). Importantly, Dynole-34-2 (Figure 4), MitMAB (Figure 5) and dynasore (results not shown) inhibited syncytium formation when added after the end of the low pH pulse. Taking into account that by this time early fusion stages that yield nascent fusion pores had taken place [14,15,45], these findings suggested that the inhibition of the GTPase activity of dynamin blocked the late stages of syncytium formation. Indeed, we found that neither Dynole-34-2 (Figure 4) nor dynasore (results not shown) inhibited lipid mixing in a gp64-mediated fusion.

To explore further the involvement of dynamin in syncytium formation, we infected Sf9 cells with baculoviruses encoding different dominant-negative human dynamin-1 mutants. In contrast with Sf^{Op1D} cells that constitutively express the protein fusogen gp64, Sf9 cells expressed gp64 as a result of baculovirus infection. We adjusted the concentrations of all of the baculovirus constructs used to achieve similar levels of gp64 expression (detected by a cELISA, Supplementary Figure S2; and by Western

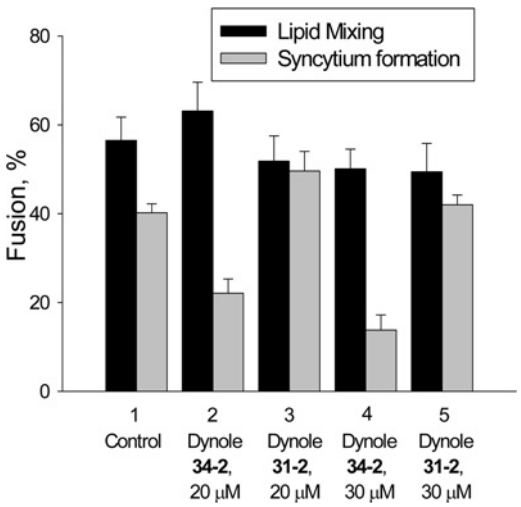

Figure 4 Dynole-34-2, an inhibitor of dynamin GTPase activity, inhibits gp64-initiated syncytium formation, but does not inhibit lipid mixing

Dynole-34-2 (bars 2 and 4) or its inactive derivative Dynole-31-2 (bars 3 and 5) was applied to Sf9^{Op1D} cells (final concentration 20 μM, bars 2 and 3 or 30 μM, bars 4 and 5) immediately after a 1 min application of pH 4.9 medium. (1) Control with no reagents applied. Final extents of lipid mixing and syncytium formation (black and grey bars respectively) were measured 20 min later. Results are means + S.E.M. ($n \geqslant 3$).

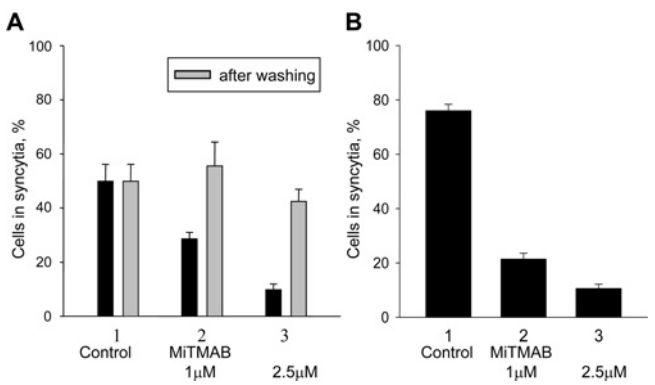

Figure 5 Blocking dynamin GTPase activity with MiTMAB applied after the end of low pH application inhibits syncytium formation initiated by either gp64 (A) or HA (B)

(**A**) Sf9^{Op1D} cells were treated with MitMAB at a final concentration of 1 μM (2) or 2.5 μM (3) (black bars). The grey bars represent the results after washing away MitMAB, restoring syncytium formation rates as in the control. (1) Control with no reagents applied. Bars are means + S.E.M. (**B**) HAb2 cells were treated with MiTMAB at final concentrations of 1 μM (2) or 2.5 μM (3). (1) Control with no reagents applied. Results are means + S.E.M. ($n \geqslant 3$).

blotting, results not shown) at the time of fusion experiments. Expression of the dynamin mutants S61D, with reduced GTPase activity [40], and I690K, with impaired self-assembly [41], lowered the extents of syncytium formation when compared with those observed for the Sf9 cells infected with wild-type baculovirus or a baculovirus construct expressing wild-type dynamin (Figure 6). Intriguingly, expression of K44A and S45N dynamin mutants defective in GTP binding [42–44] promoted syncytium formation. The effects of diverse dynamin-targeting reagents (GTPase inhibitors and dominant-negative mutants) on cell fusion reveal the importance of dynamin and dynamin partners in syncytium formation.

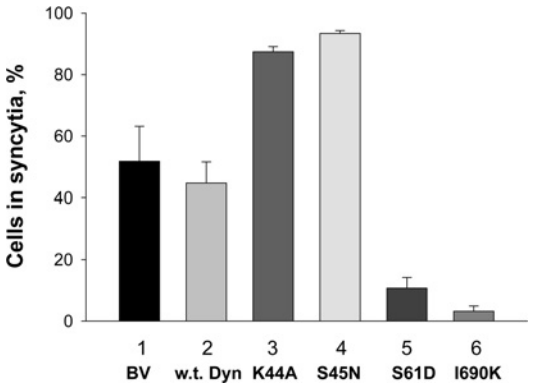

Figure 6 Different dominant-negative dynamin mutants affect gp64-initiated syncytium formation

Before inducing fusion, Sf9 cells were infected with either wild-type baculovirus (1); or baculovirus constructs expressing wild-type dynamin (2) or different dynamin mutants (3–6). (3) and (4) K44A and S45N respectively, both defective in GTP binding. (5) S61D, defective in GTP hydrolysis but not in GTP binding. (6) I690K, with impaired self-assembly. Results are means + S.E.M.

PtdIns(4,5)P_2 regulation of syncytium formation

Many CGPs, including the BAR, F-BAR and ENTH domain proteins and dynamin are recruited to the plasma membrane at least partially by binding to PtdIns(4,5)P_2 in the inner membrane leaflet. Lowering the concentrations of PtdIns(4,5)P_2 available for interactions with its endogenous effectors by three different PtdIns(4,5)P_2-targeting reagents inhibited syncytium formation. Butan-1-ol reduces stimulation of PtdIns 5-kinase, which generates PtdIns(4,5)P_2 and thus lowers PtdIns(4,5)P_2 content in the plasma membrane [51]. PtdIns(4,5)P_2 depletion by applying butan-1-ol inhibited syncytium formation (Figure 7A). In control experiments, *t*-butanol, which does not inhibit PtdIns 5-kinase, had no effect on syncytium formation. Note that, since butan-1-ol depletes PtdIns(4,5)P_2 by lowering the concentration of phosphatidic acid, an important signalling lipid, effects independent of PtdIns(4,5)P_2 cannot be excluded.

In another experimental approach, we transfected Sf9^{Op1D} cells to express the PLCδ1PH–GFP fusion protein. This protein is routinely used to visualize PtdIns(4,5)P_2 but affects PtdIns(4,5)P_2-dependent processes at high levels of expression [52]. As seen in Figure 7(B), PLCδ1PH–GFP expression inhibited syncytium formation by Sf9^{Op1D} cells, as compared with that observed for the cells transfected with the non-lipid-binding PLCδ1PH–GFP mutant R40L [39].

In our third approach, we used PBP10, a cell-permeant rhodamine-tagged decapeptide from the PtdIns(4,5)P_2-binding region of gelsolin. This peptide, known to potently bind PtdIns(4,5)P_2 and affect PtdIns(4,5)P_2-dependent processes [38], inhibited syncytium formation (Figure 7C).

To summarize, lowering the concentration of plasma membrane PtdIns(4,5)P_2 accessible for interactions with CGPs [and other PtdIns(4,5)P_2-binding proteins] inhibits syncytium formation. Since both PBP10 and butan-1-ol were applied after a low pH pulse, our findings indicate that PtdIns(4,5)P_2 content and accessibility are important for late fusion stages.

DISCUSSION

In the present study, we have explored the late stages of cell–cell fusion in which the nascent fusion pore(s) generated by viral fusogens baculovirus gp64 and influenza HA expand(s) to form

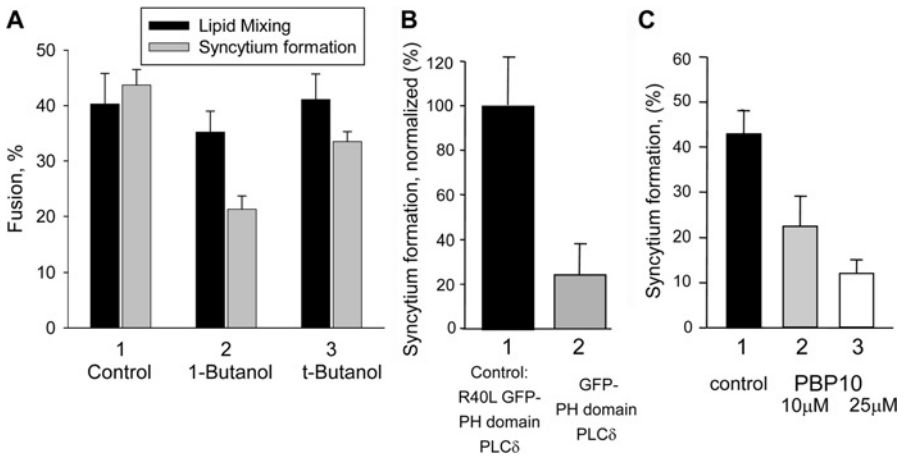

Figure 7 Inhibition of gp64-initiated syncytium formation by lowering the concentration of accessible PtdIns(4,5)P_2 in the plasma membrane

(**A**) Butan-1-ol application to $Sf9^{0p1D}$ cells immediately after the end of low pH application inhibited syncytium formation (grey bars), but had no effect on lipid mixing (black bars). In control experiments, the cells were treated with *t*-butanol that, in contrast with butan-1-ol, does not induce PtdIns(4,5)P_2 depletion. (**B**) Expression of the PLCδ1PH–GFP construct in $Sf9^{0p1D}$ cells inhibited cell fusion that was triggered 24 h post-transfection. Syncytium formation for the cells expressing PLCδ1PH–GFP was normalized to that observed for the cells expressing the PLCδ1PH–GFP mutant R40L. (**C**) Inhibition of syncytium formation by $Sf9^{0p1D}$ cells by PBP10 (10 or 25 μM, bars 2 and 3) applied immediately after the end of low pH application. (1) Control with no reagents applied. For (**A**), (**B**) and (**C**), fusion between $Sf9^{0p1D}$ cells was triggered by a 1 min application of pH 4.9 medium and assayed 20 min later. Results are means + S.E.M.

syncytia. Fusion pores that develop with a tight contact between cell membranes have a strongly bent rim accumulating the elastic energy of membrane bending. Thus the pore expansion is an energy-consuming process. Earlier studies indicated that the enlargement of micron-scale pores in syncytium formation does not proceed spontaneously but rather involves the cell machinery [12,13,53]. Neither release of membrane lateral tension nor disruption of the force generating intracellular systems such as the actin cytoskeleton and microtubular structures inhibits fusion pore expansion in syncytium formation [12,13,19,54]. We hypothesized that large fusion pores grow because the rim of the pore accumulates proteins that relax its bending energy. The shape of a fusion pore developing in a cell–cell contact zone with an inter-membrane distance of ~20 nm is similar to a half cylinder with a ~20 nm diameter [13]. Since the comparable curvature radii are characteristic for highly curved membrane compartments such as endocytic vesicles, we proposed that the late stages of fusion pore growth involve CGPs that drive intracellular membrane shaping. To test this hypothesis, in the present study we explored whether syncytium formation can be promoted by raising the intracellular concentrations of membrane-binding and -bending domains from three CGPs (GRAF1, FCHo2 and epsin) in cells by either overexpressing these proteins or by microinjecting them. Indeed, these diverse CGPs (with BAR, F-BAR and ENTH domains) promoted the late stages of HA-initiated cell-to-cell fusion. Note that, although this finding is consistent with our hypothesis as a proof of principle, the specific different CGPs that may have the most potent effect in fusion between HAb2 cells or other cells remain to be identified. A recent study indicates that GRAF1 expression in C2C12 cells promotes both myogenic differentiation and fusion between differentiated myoblasts [55]. GRAF1-dependent promotion of cell fusion is suggested to involve BAR domain-mediated membrane sculpting. Our findings in a much simpler experimental system are consistent with this mechanism and suggest that it acts downstream of early fusion stages at a stage of fusion pore expansion.

The conclusion that late stages of syncytium formation involve CGPs was strengthened further by experiments with reagents targeting the function of one of the most abundant CGPs: dynamin [22,23]. Both free dynamin tetramers and membrane associated dimers, the building blocks of larger oligomers, are rigid elongated structures with a curved shape. Curvature generated by dynamin can result in different membrane shapes. Long helical oligomers constrain the membrane into tubular shapes. Oligomers that are too short to form helices can generate a wider variety of shapes which include tubular and spherical shapes. Blocking of the GTPase activity of dynamin by dynasore [35], MiTMAB [36] and Dynole-34-2 [37] inhibited syncytium formation initiated by either HA or gp64. Dynamin inhibitors did not inhibit lipid mixing and blocked syncytium formation even when applied after a low pH pulse application, that is, at the time when both HA [56] and, especially, gp64 [14] have already formed initial fusion pores. Thus dynamin plays its role downstream of the opening of fusion pores. Our findings suggest that the recently reported inhibition of HIV env-mediated cell–cell fusion by dynasore [57] also reflects dynamin-dependence of late, rather than early, fusion stages.

Dominant-negative dynamin mutants also affected cell-to-cell fusion. Similar to the experiments using inhibitors, syncytium formation was inhibited by stabilization of the GTP-bound form of dynamin by overexpressing a GTPase-defective S61D mutant [40]. Syncytium formation was also inhibited by the assembly-defective I690K mutant of dynamin, which is impaired in membrane surface affinity [41]. In contrast, K44A and S45N, two mutants of dynamin defective in GTP binding [42–44], promoted syncytium formation. This promotion may indicate that GTP-free dynamins are more likely than GTP–dynamins to form short arc-like oligomers that facilitate fusion pore expansion. However, this hypothesis remains to be tested. Importantly, since impaired GTP binding for these mutants inhibits GTP hydrolysis, the promotion of syncytium formation argues against the hypothesis that fusion pore expansion is somehow driven by the energy derived from the GTP hydrolysis by dynamin.

The finding that diverse dynamin-targeting reagents have notable effects on the efficiency of syncytium formation suggests the involvement of dynamin in cell–cell fusion. However, although the ability of dynamin to shape membranes is well documented, we cannot at the present time offer a specific mechanism by which curvature generation by dynamin promotes fusion pore expansion. In one scenario, dynamin oligomers, too short to form complete circles or helices and thus shaped as open

arcs bind to the curved membrane of a nascent fusion pore rim. Owing to their ability to generate membrane curvature similar to that of the pore edge, binding of these arc-like oligomers drives expansion of the pore edge by bending additional portions of the initially flat membrane of the intracellular contact into the bent shape of the pore rim. Stabilization of the GTP-bound form of dynamin may promote the formation of the long helical structures and therefore the membrane tubules. As mentioned above, short oligomers can be accommodated both in tubules and in the fusion pore rim, and thus competition between the tubules and pore rim for the short-arc dynamins is expected to deplete the pool of short oligomers in the rim and inhibit pore expansion. Further research will either further develop this mechanism to explain the specific effects of different dynamin mutants or bring about alternative mechanisms that may couple membrane shaping by dynamin with fusion pore expansion at late stages of cell-to-cell fusion. Importantly, since dynamin both directly and via interactions with other proteins regulates many different processes in cell physiology, the role of dynamin in syncytium formation might be complex and indirect.

The activity of many intracellular CGPs is regulated by polyphosphoinositides. The present study is the first demonstration that PtdIns(4,5)P_2 content controls syncytium formation. Inhibition of the late stages of cell fusion by lowering the concentration of accessible PtdIns(4,5)P_2 in the plasma membrane is consistent with the hypothesis that CGPs drive the expansion of fusion pores. However, PtdIns(4,5)P_2 can also affect late fusion stages by regulating PtdIns(4,5)P_2-binding proteins other than CGPs.

To conclude, the late stages of cell-to-cell fusion initiated by well-characterized viral fusogens depend on the functional activity of intracellular CGPs, including dynamin and representatives of the BAR, F-BAR and ENTH protein families. However, a number of important questions remain open. To start with, the mechanism underlying this dependence is yet to be clarified. CGPs can directly facilitate fusion pore expansion by accumulating at the pore edge and lowering its energy. In principle, CGPs can also promote vesiculation of the membrane junction at the edge of the fusion pores [33]. However, at least in the case of gp64-initiated fusion of Sf9 cells, fusion pores appear to grow by the displacement of membrane material towards the periphery of the contact zone rather than by vesiculation [13]. The analysis of the role of CGPs in syncytium formation also has to be extended to biologically important examples of cell fusion such as fusion between myoblasts and between macrophages, and then to the identification of specific CGPs involved in these processes. Better understanding of the mechanism and cell machinery responsible for driving fusion pore expansion in cell-to-cell fusion will bring about new ways of controlling fusion in development and in pathological conditions. The dependence of fusion pore expansion on cell machinery can also be of importance for understanding why transient nanotubular connections between plasma membranes of some cells [58,59] do not expand to yield multinucleated cells.

The present study emphasizes an interesting overlap between proteins controlling the late stages of cell-to-cell fusion and proteins that drive the oppositely directed process of membrane remodelling, the fission of one cell membrane into two. Dynamin and curvature-generating domains of GRAF1, FCHo2 and epsin that we found to influence syncytium formation are essential components of different endocytic pathways [23–25,27,28,30] that culminate in membrane fission. Proteins of the dynamin family have been also implicated in mitochondrial fusion [60,61] and fusion of ER membranes [62,63]. Dynamin is involved in an as yet unclear mechanism in HIV fusion with the endosomal membrane, as suggested by a fusion inhibition using the dynamin GTPase inhibitor dynasore [64]. Furthermore, dynasore promotes the release of luminal and membrane biosynthetic cargoes from individual post-Golgi vesicles, suggesting that dynamin redirects fusion pore evolution from expansion to premature closure in 'kiss-and-run' exocytosis [65]. A recent study confirms that dynamin regulates the rapidity of fusion pore expansion in exocytosis and suggests that dynamin assembly restricts fusion pore expansion until GTP-hydrolysis-stimulated disassembly [66]. Another component of the endocytic machinery, the BAR domain protein amphiphysin, has also been reported to restrict dilation of fusion pores [67]. Note that, in terms of membrane curvature and positioning of proteins, the closing of the exocytotic fusion pore by CGPs (dynamin [65] and amphiphysin [67]) located outside of the pore lumen is topologically similar to fusion pore expansion in syncytium formation by the proteins located inside the lumen of the pore. Further elucidation of the overlap between the protein players involved in the processes that unite and divide biological membranes is important for finding shared mechanistic principles underlying fusion and fission [68]. Although our results from the present study demonstrate that different CGPs can control the expansion of fusion pores, we still do not know which of the diverse intracellular CGPs control these stages in biologically important cell-to-cell fusion processes. Our finding that increases in concentration of either of the several CGP domains promote transition from early fusion intermediates to syncytium formation suggests a redundancy of their membrane-bending function.

AUTHOR CONTRIBUTION

Jean-Philippe Richard, Evgenia Leikina, Michael Kozlov and Leonid Chernomordik conceived and planned the experiments. Jean-Philippe Richard, Evgenia Leikina and Margarita Popova carried out the experiments and analysed the data. Ralf Langen, Tamas Balla, Harvey McMahon and William Mike Henne advised on specific aspects of the experimental strategies and provided constructs and proteins. Leonid Chernomordik, Jean-Philippe Richard and Michael Kozlov wrote the paper.

ACKNOWLEDGEMENTS

We are indebted to Dr S. Schmid (The Scripps Research Institute) and Dr T. Kirchhausen for dynamin constructs and dynasore respectively. We thank Dr K. Melikov and Dr J. Zimmerberg for very helpful discussions prior to submission.

FUNDING

The research was supported by the Intramural Research Program of the Eunice Kennedy Shriver National Institute of Child Health and Human Development, National Institutes of Health and an National Institute of Allergy and Infectious Diseases, National Institutes of Health Intramural Biodefense Research grant (both to L.V.C.) and by the National Institutes of Health [grant number 2 R01 GM063915 (to R.L.)].

REFERENCES

1 Jahn, R., Lang, T. and Sudhof, T. C. (2003) Membrane fusion. Cell **112**, 519–533
2 Earp, L. J., Delos, S. E., Park, H. E. and White, J. M. (2005) The many mechanisms of viral membrane fusion proteins. Curr. Top. Microbiol. Immunol. **285**, 25–66
3 Chen, E. H., Grote, E., Mohler, W. and Vignery, A. (2007) Cell-cell fusion. FEBS Lett. **581**, 2181–2193
4 Duelli, D. and Lazebnik, Y. (2007) Cell-to-cell fusion as a link between viruses and cancer. Nat. Rev. Cancer **7**, 968–976
5 Sapir, A., Avinoam, O., Podbilewicz, B. and Chernomordik, L. V. (2008) Viral and developmental cell fusion mechanisms: conservation and divergence. Dev. Cell **14**, 11–21
6 Kielian, M. and Rey, F. A. (2006) Virus membrane-fusion proteins: more than one way to make a hairpin. Nat. Rev. Microbiol. **4**, 67–76
7 Weissenhorn, W., Hinz, A. and Gaudin, Y. (2007) Virus membrane fusion. FEBS Lett. **581**, 2150–2155

8 Martens, S. and McMahon, H. T. (2008) Mechanisms of membrane fusion: disparate players and common principles. Nat. Rev. Mol. Cell Biol. **9**, 543–556
9 Cohen, F. S. and Melikyan, G. B. (2004) The energetics of membrane fusion from binding, through hemifusion, pore formation, and pore enlargement. J. Membr. Biol. **199**, 1–14
10 Chernomordik, L. V., Zimmerberg, J. and Kozlov, M. M. (2006) Membranes of the world unite. J. Cell Biol. **175**, 201–207
11 Jackson, M. B. and Chapman, E. R. (2008) The fusion pores of Ca^{2+}-triggered exocytosis. Nat. Struct. Mol. Biol. **15**, 684–689
12 Richard, J. P., Leikina, E. and Chernomordik, L. V. (2009) Cytoskeleton reorganization in influenza hemagglutinin-initiated syncytium formation. Biochim. Biophys. Acta **1788**, 450–457
13 Chen, A., Leikina, E., Melikov, K., Podbilewicz, B., Kozlov, M. M. and Chernomordik, L. V. (2008) Fusion-pore expansion during syncytium formation is restricted by an actin network. J. Cell Sci. **121**, 3619–3628
14 Plonsky, I. and Zimmerberg, J. (1996) The initial fusion pore induced by baculovirus GP64 is large and forms quickly. J. Cell Biol. **135**, 1831–1839
15 Zimmerberg, J., Blumenthal, R., Sarkar, D. P., Curran, M. and Morris, S. J. (1994) Restricted movement of lipid and aqueous dyes through pores formed by influenza hemagglutinin during cell fusion. J. Cell Biol. **127**, 1885–1894
16 Zheng, Q. A. and Chang, D. C. (1991) Reorganization of cytoplasmic structures during cell fusion. J. Cell Sci. **100**, 431–442
17 Massarwa, R., Carmon, S., Shilo, B. Z. and Schejter, E. D. (2007) WIP/WASp-based actin-polymerization machinery is essential for myoblast fusion in *Drosophila*. Dev. Cell **12**, 557–569
18 Gildor, B., Massarwa, R., Shilo, B. Z. and Schejter, E. D. (2009) The SCAR and WASp nucleation-promoting factors act sequentially to mediate *Drosophila* myoblast fusion. EMBO Rep. **10**, 1043–1050
19 Wurth, M. A., Schowalter, R. M., Smith, E. C., Moncman, C. L., Dutch, R. E. and McCann, R. O. (2010) The actin cytoskeleton inhibits pore expansion during PIV5 fusion protein-promoted cell-cell fusion. Virology **404**, 117–126
20 Dawson, J. C., Legg, J. A. and Machesky, L. M. (2006) Bar domain proteins: a role in tubulation, scission and actin assembly in clathrin-mediated endocytosis. Trends Cell Biol. **16**, 493–498
21 Doherty, G. J. and McMahon, H. T. (2008) Mediation, modulation, and consequences of membrane-cytoskeleton interactions. Annu. Rev. Biophys. **37**, 65–95
22 Hinshaw, J. E. (2000) Dynamin and its role in membrane fission. Annu. Rev. Cell Dev. Biol. **16**, 483–519
23 Praefcke, G. J. and McMahon, H. T. (2004) The dynamin superfamily: universal membrane tubulation and fission molecules? Nat. Rev. Mol. Cell Biol. **5**, 133–147
24 Mettlen, M., Pucadyil, T., Ramachandran, R. and Schmid, S. L. (2009) Dissecting dynamin's role in clathrin-mediated endocytosis. Biochem. Soc. Trans. **37**, 1022–1026
25 Ford, M. G., Mills, I. G., Peter, B. J., Vallis, Y., Praefcke, G. J., Evans, P. R. and McMahon, H. T. (2002) Curvature of clathrin-coated pits driven by epsin. Nature **419**, 361–366
26 Itoh, T. and De Camilli, P. (2006) BAR, F-BAR (EFC) and ENTH/ANTH domains in the regulation of membrane-cytosol interfaces and membrane curvature. Biochim. Biophys. Acta **1761**, 897–912
27 Doherty, G. J. and Lundmark, R. (2009) GRAF1-dependent endocytosis. Biochem. Soc. Trans. **37**, 1061–1065
28 Lundmark, R., Doherty, G. J., Howes, M. T., Cortese, K., Vallis, Y., Parton, R. G. and McMahon, H. T. (2008) The GTPase-activating protein GRAF1 regulates the CLIC/GEEC endocytic pathway. Curr. Biol. **18**, 1802–1808
29 Lundmark, R. and Carlsson, S. R. (2010) Driving membrane curvature in clathrin-dependent and clathrin-independent endocytosis. Semin. Cell Dev. Biol. **21**, 363–370
30 Henne, W. M., Boucrot, E., Meinecke, M., Evergren, E., Vallis, Y., Mittal, R. and McMahon, H. T. (2010) FCHo proteins are nucleators of clathrin-mediated endocytosis. Science **328**, 1281–1284
31 Takenawa, T. (2010) Phosphoinositide-binding interface proteins involved in shaping cell membranes. Proc. Jpn. Acad., Ser. B **86**, 509–523
32 Doberstein, S. K., Fetter, R. D., Mehta, A. Y. and Goodman, C. S. (1997) Genetic analysis of myoblast fusion: blown fuse is required for progression beyond the prefusion complex. J. Cell Biol. **136**, 1249–1261
33 Mohler, W. A., Simske, J. S., Williams-Masson, E. M., Hardin, J. D. and White, J. G. (1998) Dynamics and ultrastructure of developmental cell fusions in the *Caenorhabditis elegans* hypodermis. Curr. Biol. **8**, 1087–1090
34 Sens, K. L., Zhang, S., Jin, P., Duan, R., Zhang, G., Luo, F., Parachini, L. and Chen, E. H. (2010) An invasive podosome-like structure promotes fusion pore formation during myoblast fusion. J. Cell Biol. **191**, 1013–1027
35 Macia, E., Ehrlich, M., Massol, R., Boucrot, E., Brunner, C. and Kirchhausen, T. (2006) Dynasore, a cell-permeable inhibitor of dynamin. Dev. Cell **10**, 839–850
36 Quan, A., McGeachie, A. B., Keating, D. J., van Dam, E. M., Rusak, J., Chau, N., Malladi, C. S., Chen, C., McCluskey, A., Cousin, M. A. and Robinson, P. J. (2007) Myristyl trimethyl ammonium bromide and octadecyl trimethyl ammonium bromide are surface-active small molecule dynamin inhibitors that block endocytosis mediated by dynamin I or dynamin II. Mol. Pharmacol. **72**, 1425–1439
37 Hill, T. A., Gordon, C. P., McGeachie, A. B., Venn-Brown, B., Odell, L. R., Chau, N., Quan, A., Mariana, A., Sakoff, J. A., Chircop, M. et al. (2009) Inhibition of dynamin mediated endocytosis by the dynoles–synthesis and functional activity of a family of indoles. J. Med. Chem. **52**, 3762–3773
38 Cunningham, C. C., Vegners, R., Bucki, R., Funaki, M., Korde, N., Hartwig, J. H., Stossel, T. P. and Janmey, P. A. (2001) Cell permeant polyphosphoinositide-binding peptides that block cell motility and actin assembly. J. Biol. Chem. **276**, 43390–43399
39 Holz, R. W., Hlubek, M. D., Sorensen, S. D., Fisher, S. K., Balla, T., Ozaki, S., Prestwich, G. D., Stuenkel, E. L. and Bittner, M. A. (2000) A pleckstrin homology domain specific for phosphatidylinositol 4, 5-bisphosphate (PtdIns-4,5-P_2) and fused to green fluorescent protein identifies plasma membrane PtdIns-4,5-P_2 as being important in exocytosis. J. Biol. Chem. **275**, 17878–17885
40 Song, B. D., Leonard, M. and Schmid, S. L. (2004) Dynamin GTPase domain mutants that differentially affect GTP binding, GTP hydrolysis, and clathrin-mediated endocytosis. J. Biol. Chem. **279**, 40431–40436
41 Song, B. D., Yarar, D. and Schmid, S. L. (2004) An assembly-incompetent mutant establishes a requirement for dynamin self-assembly in clathrin-mediated endocytosis *in vivo*. Mol. Biol. Cell **15**, 2243–2252
42 Damke, H., Baba, T., Warnock, D. E. and Schmid, S. L. (1994) Induction of mutant dynamin specifically blocks endocytic coated vesicle formation. J. Cell Biol. **127**, 915–934
43 Damke, H., Binns, D. D., Ueda, H., Schmid, S. L. and Baba, T. (2001) Dynamin GTPase domain mutants block endocytic vesicle formation at morphologically distinct stages. Mol. Biol. Cell **12**, 2578–2589
44 Marks, B., Stowell, M. H., Vallis, Y., Mills, I. G., Gibson, A., Hopkins, C. R. and McMahon, H. T. (2001) GTPase activity of dynamin and resulting conformation change are essential for endocytosis. Nature **410**, 231–235
45 Chernomordik, L. V., Frolov, V. A., Leikina, E., Bronk, P. and Zimmerberg, J. (1998) The pathway of membrane fusion catalyzed by influenza hemagglutinin: restriction of lipids, hemifusion, and lipidic fusion pore formation. J. Cell Biol. **140**, 1369–1382
46 Plonsky, I., Cho, M. S., Oomens, A. G., Blissard, G. and Zimmerberg, J. (1999) An analysis of the role of the target membrane on the Gp64-induced fusion pore. Virology **253**, 65–76
47 Chernomordik, L., Leikina, E. and Zimmerberg, J. (1995) Control of baculovirus gp64-induced syncytia formation by membrane lipid composition. J. Virol. **69**, 3049–3058
48 Markovic, I., Leikina, E., Zhukovsky, M., Zimmerberg, J. and Chernomordik, L. V. (2001) Synchronized activation and refolding of influenza hemagglutinin in multimeric fusion machines. J. Cell Biol. **155**, 833–844
49 Henne, W. M., Kent, H. M., Ford, M. G., Hegde, B. G., Daumke, O., Butler, P. J., Mittal, R., Langen, R., Evans, P. R. and McMahon, H. T. (2007) Structure and analysis of FCHo2 F-BAR domain: a dimerizing and membrane recruitment module that effects membrane curvature. Structure **15**, 839–852
50 Kruchten, A. E. and McNiven, M. A. (2006) Dynamin as a mover and pincher during cell migration and invasion. J. Cell Sci. **119**, 1683–1690
51 Boucrot, E., Saffarian, S., Massol, R., Kirchhausen, T. and Ehrlich, M. (2006) Role of lipids and actin in the formation of clathrin-coated pits. Exp. Cell Res. **312**, 4036–4048
52 Balla, T. and Varnai, P. (2009) Visualization of cellular phosphoinositide pools with GFP-fused protein-domains. Curr. Protoc. Cell Biol. **24**, 24.4
53 Kempf, C., Kohler, U., Michel, M. R. and Koblet, H. (1987) Semliki Forest virus-induced polykaryocyte formation is an ATP-dependent event. Arch. Virol. **95**, 111–122
54 Wang, E., Cross, R. K. and Choppin, P. W. (1979) Involvement of microtubules and 10-nm filaments in the movement and positioning of nuclei in syncytia. J. Cell Biol. **83**, 320–337
55 Doherty, J., Lenhart, K., Cameron, M., Mack, C., Conlon, F. and Taylor, J. (2011) Skeletal muscle differentiation and fusion is regulated by the BAR-containing Rho GAP, GRAF1. J. Biol. Chem. **286**, 25903–25921
56 Mittal, A., Leikina, E., Chernomordik, L. V. and Bentz, J. (2003) Kinetically differentiating influenza hemagglutinin fusion and hemifusion machines. Biophys. J. **85**, 1713–1724
57 Lai, W., Huang, L., Ho, P., Montefiori, D. and Chen, C. H. (2011) The role of dynamin in HIV type 1 env-mediated cell-cell fusion. AIDS Res. Hum. Retroviruses **27**, 1013–1017
58 Rustom, A., Saffrich, R., Markovic, I., Walther, P. and Gerdes, H. H. (2004) Nanotubular highways for intercellular organelle transport. Science **303**, 1007–1010
59 Niu, X., Gupta, K., Yang, J. T., Shamblott, M. J. and Levchenko, A. (2009) Physical transfer of membrane and cytoplasmic components as a general mechanism of cell-cell communication. J. Cell Sci. **122**, 600–610
60 Hoppins, S., Lackner, L. and Nunnari, J. (2007) The machines that divide and fuse mitochondria. Annu. Rev. Biochem. **76**, 751–780

61 Hoppins, S. and Nunnari, J. (2009) The molecular mechanism of mitochondrial fusion. Biochim. Biophys. Acta **1793**, 20–26
62 Hu, J., Shibata, Y., Zhu, P. P., Voss, C., Rismanchi, N., Prinz, W. A., Rapoport, T. A. and Blackstone, C. (2009) A class of dynamin-like GTPases involved in the generation of the tubular ER network. Cell **138**, 549–561
63 Orso, G., Pendin, D., Liu, S., Tosetto, J., Moss, T. J., Faust, J. E., Micaroni, M., Egorova, A., Martinuzzi, A., McNew, J. A. and Daga, A. (2009) Homotypic fusion of ER membranes requires the dynamin-like GTPase atlastin. Nature **460**, 978–983
64 Miyauchi, K., Kim, Y., Latinovic, O., Morozov, V. and Melikyan, G. B. (2009) HIV enters cells via endocytosis and dynamin-dependent fusion with endosomes. Cell **137**, 433–444
65 Jaiswal, J. K., Rivera, V. M. and Simon, S. M. (2009) Exocytosis of post-Golgi vesicles is regulated by components of the endocytic machinery. Cell **137**, 1308–1319
66 Anantharam, A., Bittner, M. A., Aikman, R. L., Stuenkel, E. L., Schmid, S. L., Axelrod, D. and Holz, R. W. (2011) A new role for the dynamin GTPase in the regulation of fusion pore expansion. Mol. Biol. Cell **22**, 1907–1918
67 Llobet, A., Wu, M. and Lagnado, L. (2008) The mouth of a dense-core vesicle opens and closes in a concerted action regulated by calcium and amphiphysin. J. Cell Biol. **182**, 1017–1028
68 Kozlov, M. M., McMahon, H. T. and Chernomordik, L. V. (2010) Protein-driven membrane stresses in fusion and fission. Trends Biochem. Sci. **35**, 699–706

Received 11 July 2011/18 August 2011; accepted 7 September 2011
Published as BJ Immediate Publication 7 September 2011, doi:10.1042/BJ20111243

Biochem. J. (2011) **440**, 185–193 (Printed in Great Britain) doi:10.1042/BJ20111243

online data

SUPPLEMENTARY ONLINE DATA

Intracellular curvature-generating proteins in cell-to-cell fusion

Jean-Philippe RICHARD*[1,2], Evgenia LEIKINA*[1], Ralf LANGEN†, William Mike HENNE‡[3], Margarita POPOVA*, Tamas BALLA§, Harvey T. McMAHON‡, Michael M. KOZLOV‖ and Leonid V. CHERNOMORDIK*[4]

*Section on Membrane Biology, Laboratory of Cellular and Molecular Biophysics, Eunice Kennedy Shriver National Institute of Child Health and Human Development, National Institutes of Health, 10 Center Dr., Bethesda, MD 20892-1855, U.S.A., †Zilkha Neurogenetic Institute and Department of Biochemistry, Keck School of Medicine, University of Southern California, Los Angeles, CA 90033, U.S.A., ‡MRC Laboratory of Molecular Biology, Hills Road, Cambridge CB2 0QH, U.K., §Section on Molecular Signal Transduction, Program for Developmental Neuroscience, National Institute of Child Health and Human Development, National Institutes of Health, Bethesda, MD 20892, U.S.A., and ‖Department of Physiology and Pharmacology, Sackler Faculty of Medicine, Tel Aviv University, 69978 Tel Aviv, Israel

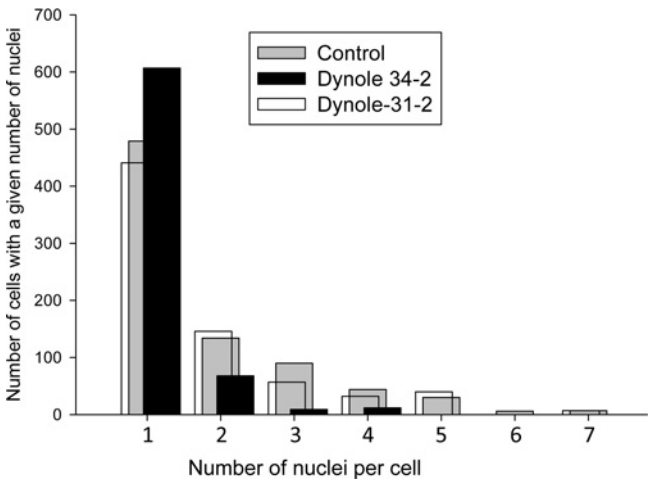

Figure S1 Dynole-34-2, an inhibitor of dynamin GTPase activity, decreases the sizes of syncytia formed by $Sf9^{0p1D}$ cells

Dynole-34-2 (black bars) or its inactive derivative Dynole-31-2 (open bars) was applied to $Sf9^{0p1D}$ cells (final concentrations of 30 μM) immediately after a 1 min application of pH 4.9 medium. Grey bars indicate control with no reagents applied. Syncytium formation was evaluated 20 min later by counting the numbers of cells containing different numbers of nuclei (from one to seven).

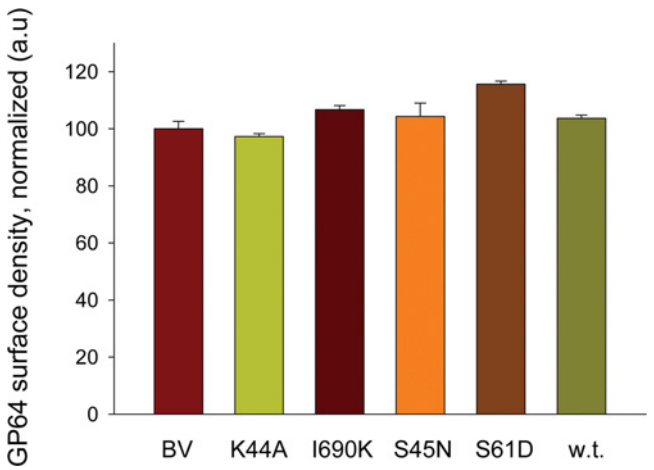

Figure S2 Cell-surface density of baculovirus gp64 in the experiments with Sf9 cells infected with either wild-type baculovirus (BV) or baculovirus constructs expressing wild-type dynamin (w.t.) or different dynamin mutants (K44A, I690K, S45N and S61D)

The surface expression of gp64 was evaluated 2 days post-infection by cELISA. Results are means + S.E.M.

Received 11 July 2011/18 August 2011; accepted 7 September 2011
Published as BJ Immediate Publication 7 September 2011, doi:10.1042/BJ20111243

[1] These authors contributed equally to this work
[2] Present address: Hugo W. Moser Research Institute at Kennedy Krieger, Department of Neurology, Johns Hopkins School of Medicine, Baltimore, MD 21205, U.S.A.
[3] Present address: Weill Institute for Cell and Molecular Biology, Cornell University, Ithaca, NY 14853, U.S.A.
[4] To whom correspondence should be addressed (email chernoml@mail.nih.gov).